



**HAL**  
open science

## Direct determination of free metal concentration by implementing stripping chronopotentiometry as the second stage of AGNES

Corinne Parat, Laurent Authier, D. Aguilar, E. Companys, J. Puy, J. Galceran, Martine Potin-Gautier

### ► To cite this version:

Corinne Parat, Laurent Authier, D. Aguilar, E. Companys, J. Puy, et al.. Direct determination of free metal concentration by implementing stripping chronopotentiometry as the second stage of AGNES. *Analyst*, 2011, 136 (20), pp.4337-4343. 10.1039/c1an15481h . hal-01444584

**HAL Id: hal-01444584**

**<https://hal.science/hal-01444584>**

Submitted on 14 Mar 2018

**HAL** is a multi-disciplinary open access archive for the deposit and dissemination of scientific research documents, whether they are published or not. The documents may come from teaching and research institutions in France or abroad, or from public or private research centers.

L'archive ouverte pluridisciplinaire **HAL**, est destinée au dépôt et à la diffusion de documents scientifiques de niveau recherche, publiés ou non, émanant des établissements d'enseignement et de recherche français ou étrangers, des laboratoires publics ou privés.

1 **Direct determination of free metal concentration by**  
2 **implementing stripping chronopotentiometry as second stage**  
3 **of AGNES**

4

5 C. Parat <sup>a\*</sup>, L. Authier <sup>a</sup>, D. Aguilar <sup>b</sup>, E. Companys <sup>b</sup>, J. Puy <sup>b</sup>, J. Galceran <sup>b</sup> and M.  
6 Potin-Gautier <sup>a</sup>

7 *<sup>a</sup>Université de Pau et des Pays de l'Adour, L.C.A.B.I.E., UMR 5254, IPREM, Av. P.*  
8 *Angot, 64053 Pau Cedex 9, France*

9 *<sup>b</sup>Departament de Química. Universitat de Lleida, Rovira Roure 191, 25198 Lleida,*  
10 *Spain*

11

12 \*Corresponding author. E-mail: corinne.parat@univ-pau.fr; fax: +33 559 40 76 74

13

14

15 **Abstract**

16 The electroanalytical technique Absence of Gradients and Nernstian Equilibrium  
17 Stripping (AGNES) has been extended by applying stripping chronopotentiometry  
18 (SCP) as the reoxidation stage in the determination of the free concentration of  $Zn^{2+}$ ,  
19  $Cd^{2+}$  and  $Pb^{2+}$ . This new approach, called AGNES-SCP, has been implemented with  
20 screen-printed electrodes (SPE) and the standard Hanging Mercury Drop Electrode  
21 (HMDE). Clear advantages of this variant have been shown: i) the easy resolution of the  
22 peaks of different metals present in mixtures and ii) the sparing of blanks. A rigorous  
23 computation of the faradaic charge along the SCP stage takes into account the  
24 contribution of other oxidants, which can be efficiently measured at the end of the  
25 deposition stage of AGNES. The free Cd concentration determined in an oxalate  
26 solution at pH 6 with an HMDE as working electrode agreed well with values obtained  
27 with a Cd Ion Selective Electrode. The free metal concentration measured using an SPE  
28 for the system Cd and nitrilotriacetic acid (NTA) at pH=4.8 conformed also well with  
29 Visual Minteq results.

30

31 **Keywords:** Screen-Printed Electrodes, AGNES, stripping chronopotentiometry, trace  
32 metals, HMDE

33

## 34 **1. Introduction**

35 Over the past decades, two equilibrium models, the free ion activity model (FIAM)<sup>1</sup> and  
36 the biotic ligand model (BLM)<sup>2</sup> have been developed to predict metal bioavailability  
37 and toxicity in environmental systems. In both models, the role of free metal ion  
38 concentration can be far more important than the one of the total concentration. Thus, its  
39 determination becomes a relevant analytical goal.

40 However, to date, there is a limited number of techniques<sup>3</sup> able to determine the free ion  
41 concentration with the required selectivity and detection limit such as Donnan  
42 Membrane Technique (DMT),<sup>4</sup> Complexing gel Integrated microelectrode (CGIME),<sup>5</sup>  
43 Permeation liquid membrane (PLM)<sup>6</sup> or Potentiometry with ion selective electrode  
44 (ISE).<sup>7</sup> ISE is, in principle, an ideal method for free trace metal determination, because  
45 it does not disturb the equilibria and the sample composition during the analytical  
46 procedure. Unfortunately, commercial ISEs, which exist only for a limited number of  
47 metal ions, generally lack the required sensitivity and suffer from interferences with  
48 other metal ions. Other voltammetric techniques, such as cathodic stripping voltammetry,  
49 require involved interpretations and the knowledge of several physicochemical  
50 parameters in order to yield an estimate of the free metal ion concentrations.

51 To overcome these limitations in the measurement of free metal concentrations, the  
52 electrochemical method Absence of Gradients and Nernstian Equilibrium Stripping  
53 (AGNES) has been specifically designed and developed.<sup>8,9</sup> This method consists of two  
54 stages: i) a first deposition stage in which a reduction potential  $E_1$  is applied to  
55 accumulate reduced metal into the mercury amalgam until Nernstian and diffusion  
56 equilibrium are reached, and ii) a second (stripping) stage where a more positive  
57 potential program  $E_2$  is applied, in order to reoxidate and quantify the metal  
58 accumulated in the amalgam. Several strategies have been used for this second stage: a)

59 a constant potential step (or “pulse”) under diffusion limited conditions, to take  
60 advantage of the limiting current being independent of the properties of the solution;<sup>8</sup> b)  
61 a linear re-oxidating potential sweep;<sup>10</sup> c) or a potential step at any given re-oxidation  
62 potential.<sup>11, 12</sup> Although AGNES yields results in good agreement with speciation  
63 models<sup>13-15</sup> and has been shown to be adequate for determining the free Zn  
64 concentration in natural water samples,<sup>9, 16</sup> previous variants could be affected by the  
65 interference from other cations (e.g. Cd<sup>2+</sup> determination in the presence of Pb<sup>2+</sup>). Also,  
66 in variants a) and c), a measurement of a blank is required to subtract the non-faradaic  
67 contribution.

68 In seeking an alternative second stage which could allow a discrimination of  
69 interferences and avoid the blank measurement, classical stripping methods such as  
70 “Differential Pulse” (DP), “Square Wave” (SW) or “Stripping Chronopotentiometry”  
71 (SCP) programs can be considered. Despite the widespread use of DP or SW, they are  
72 unsuitable for the second stage of AGNES as adsorption of organic species on the  
73 electrode surface appears as one of the most serious problems to obtain reliable  
74 measurements of trace metal speciation.<sup>17-19</sup> Indeed, phenomena such as complexation  
75 or adsorption can modify the response in these techniques and, thus, the analytical  
76 signal would not be directly proportional to the accumulated metal. On the other hand,  
77 SCP seems a better candidate as it does not present these problems (i.e. in its version of  
78 “complete depletion”), measures the total accumulated reduced metal and has proved to  
79 be a successful stripping technique to acquire information on different “labile” fractions  
80 of metals.<sup>20, 21</sup> SCP distinguishes the signals corresponding to the reoxidation of  
81 different metals (e.g. Zn, Cd, Pb) and does not require any blank.

82

83 The aim of this paper is to describe the advantages of SCP as stripping method of  
84 AGNES (AGNES-SCP) for the free ion concentration determination with both HMDE  
85 and Screen-Printed Electrode (SPE). After finding suitable parameters for each kind of  
86 working electrode, calibration curves have been performed separately in synthetic  
87 solutions containing  $Zn^{2+}$ ,  $Cd^{2+}$  or  $Pb^{2+}$ , and then in a mixture of these metals.  
88 Performances of each working electrode have been determined. Finally, free metal ion  
89 concentrations have been determined in synthetic solutions containing a complexing  
90 ligand and compared with results obtained from an ion selective electrode (ISE) and/or  
91 expected results computed from Visual MINTEQ.

92

## 93 **2. Material and Methods**

### 94 **2.1 Equipment and Reagents**

95 Zn, Cd and Pb 1000 mg L<sup>-1</sup> stock solutions were obtained from Merck. Potassium  
96 nitrate was used as the inert supporting electrolyte at 0.1 mol L<sup>-1</sup> and prepared from  
97 KNO<sub>3</sub> solid purchased from Aldrich (Trace Select). Potassium oxalate and  
98 nitrilotriacetic acid (NTA) in the H<sub>3</sub>L form were used as ligands (all Fluka, analytical  
99 grade). Nitric acid (69-70%, Baker Instra-Analysed for trace metal analysis), sodium  
100 hydroxide (Baker Analysed), hydrochloric acid (Baker Instra-Analysed for trace metal  
101 analysis) were purchased from Aldrich.

102 SPE were prepared using a polystyrene support for serigraphy (Sericol), carbon  
103 commercial ink electrodag PF-407A (Acheson Colloids) and mesitylen (Aldrich). The  
104 mercury deposition on the SPE was carried out using an acetate buffer solution (0.2 mol  
105 L<sup>-1</sup>, pH = 4.6) prepared from acetic acid (Trace select), sodium acetate trihydrate (Trace  
106 select) and mercury(II) nitrate 1000 mg L<sup>-1</sup> (atomic absorption standard) (all obtained  
107 from J.T. Baker).

108 Ultrapure milli-Q water was employed in all the experiments (resistivity 18 M $\Omega$  cm).  
109 Purified water-saturated nitrogen N<sub>2</sub>(50) was used for deaeration and blanketing of  
110 solutions.

111 Voltammetric measurements were performed with an Eco Chemie Autolab PGSTAT 10  
112 potentiostat attached to a Metrohm 663 VA Stand and to a computer by means of the  
113 GPES 4.9 (Eco Chemie) software package. The working electrode was a SPE or a  
114 HMDE from Metrohm (to reduce the deposition time, the smallest drop has been  
115 chosen, which corresponds to a radius around  $r_0 = 1.41 \times 10^{-4}$  m). The auxiliary electrode  
116 was a glassy carbon electrode and the reference electrode was Ag | AgCl | KCl(3 mol L<sup>-1</sup>  
117 <sup>1</sup>), encased in a 0.1 mol L<sup>-1</sup> KNO<sub>3</sub> jacket.

118 A glass combined electrode (Orion 9103) and Cd Ion-Selective Electrode (Crison,  
119 9658) were attached to an Orion Research 720A ionanalyzer and introduced in the cell  
120 to control the pH and the Cd<sup>2+</sup> concentration, respectively. Glass jacketed cells,  
121 provided by Metrohm, were thermostated at 25.0 °C and used in all the experiments.

122

## 123 **2.2 Preparation of screen printed electrode (SPE)**

124 SPE were manually screen-printed on 1 mm-thick polystyrene plates using a  
125 commercial ink to produce an array of 8 electrodes.<sup>12, 22, 23</sup> After drying 1 hour at room  
126 temperature and 1 h at 60 °C, an insulating layer (made of polystyrene dissolved in  
127 mesitylen) was spread manually over the conductive track, leaving a working disk area  
128 of 9.6 mm<sup>2</sup> and an electrical contact.

129 Then, a thin layer of mercury was electrochemically deposited onto the electrode's  
130 surface to allow trace metal detection. First, the electrode's working surface was  
131 conditioned in a 0.2 mol L<sup>-1</sup> acetate buffer solution containing 0.83 mmol L<sup>-1</sup> Hg(NO<sub>3</sub>)<sub>2</sub>,  
132 by applying 4 cycles of cyclic voltammetry (CV) using the following conditions:

133 potential range from -0.1 V to +0.8 V, scan rate 100 mV/s, step potential 2.4 mV. The  
134 Hg film was then deposited at -1.0 V, with stirring until the charge associated to the  
135 deposited mercury ( $Q_{\text{Hg}}$ ) reached 25 mC. Assuming a uniform deposition, the  
136 corresponding thickness of the Hg film would be 400 nm. However, a previous study  
137 has shown the mercury does not form a true film but rather an assembly of micro-  
138 drops.<sup>24</sup>

139 A potential of -0.1 V was fixed in between experiments in order to prevent mercury  
140 reoxidation. A new SPE has been used every day.

141

### 142 **2.3 AGNES principles**

143 AGNES consists of two conceptual stages: a first deposition stage along which the  
144 metal ion  $M^{n+}$  from the solution is reduced to  $M^0$  which accumulates in the amalgam up  
145 to the attainment of a special situation of equilibrium by the end of it, and a second  
146 stripping stage whose aim is the quantification of the reduced metal concentration.<sup>8</sup>

147 This equilibrium can, in the simplest implementation of AGNES, be achieved by  
148 applying a potential  $E_1$ , just a few millivolts more negative than the standard formal  
149 potential of the couple  $E^{0'}$ , for a sufficiently long time  $t_1$ . A more elaborate potential  
150 program ("2 pulses") has also been suggested to reach the equilibrium faster.<sup>25</sup> In this  
151 case, the potential of the first sub-stage ( $t_{1,a}$ ) practically corresponds to diffusion limited  
152 conditions, while the potential of the second sub-stage ( $t_{1,b}$ ) corresponds to the desired  
153 preconcentration. Regardless of the number of pulses, at the end of the deposition stage,  
154 Nernstian equilibrium is reached and there is no gradient in the concentration profiles at  
155 each side of the electrode surface. Nernst equation allows the concentration ratio at each  
156 side of the mercury electrode, or gain  $Y$ , to be calculated as:



$$157 \quad Y = \frac{[M^0]}{[M^{n+}]} = \exp\left[-\frac{nF}{RT}(E_1 - E^{o'})\right] \quad (1)$$

158 being  $n$  is the number of electrons,  $F$  the Faraday constant,  $R$  the gas constant,  $T$  the  
159 temperature and  $E^{o'}$  the standard formal potential of the couple.

160 The potential corresponding to a given  $Y$  can be determined from the peak potential of a  
161 differential pulse polarogram (DPP).<sup>8</sup> The higher the gain  $Y$ , the higher the sensitivity.  
162 However, higher gains will require longer electrodeposition times to reach Nernstian  
163 equilibrium.

164 The goal of the second stage of AGNES is to measure the concentration of the reduced  
165 metal  $M^0$  inside the mercury amalgam. The response function can be the faradaic  
166 current at a fixed time  $t_2$  (e.g. 0.2 s for HMDE)<sup>8</sup> or the total faradaic charge  $Q$   
167 accumulated in the deposition stage.<sup>11, 12</sup>

168 In order to subtract the non-faradaic contributions to the current or the charge in variants  
169 a) and c) (mentioned in the Introduction), the shifted blank<sup>9</sup> has been used in this work.  
170 The shifted blank (SB) consists of applying, to the solution containing the metal, a  
171 potential program shifted to a range in which there is no analyte deposition or  
172 reoxidation and keeping the same potential jump as in the metal measurement  
173 ( $E_{1, sb} - E_{2, sb} = E_1 - E_2$ ).

174

### 175 **3. Results and discussion**

#### 176 **3.1 Implementation of AGNES-SCP for HMDE**

177 Preliminary studies have been carried out in order to establish adequate experimental  
178 conditions to apply chronopotentiometry as the stripping stage of AGNES. In SCP, the  
179 analytical signal is the time taken for reoxidation (the transition time  $\tau$ ) while applying a  
180 constant oxidising current  $I_s$ .<sup>26</sup>

181 Depending on the magnitude of  $I_s$ , the conditions prevailing during the stripping stage  
182 can range from semi-infinite linear diffusion ( $I_s t^{1/2}$  constant) to the complete depletion  
183 regime ( $I_s \tau$  constant).<sup>26</sup> These conditions have been probed for HMDE applying  
184 stripping currents from 0.01 to 100 nA. All measurements have been performed with  
185 deaerated solutions of  $c_{T,Zn} = 10 \text{ nmol L}^{-1}$  and with mechanical stirring during most of  
186 the deposition stage, in order to enhance the effectiveness of the mass transport. The  
187 first AGNES stage has been performed with a two pulse program in order to reduce the  
188 deposition time:  $E_{1,a} = -1.2070 \text{ V}$  during  $t_{1,a} = 350 \text{ s}$  and  $E_{1,b} = -1.0502 \text{ V}$ , which  
189 corresponded to a gain  $Y = 500$ , during  $t_{1,b} = 1050 \text{ s}$ .<sup>25</sup> Fig. 1A shows that whatever  $I_s$ ,  
190 the product  $I_s t^{1/2}$  never attains a constant value indicating that diffusion limited  
191 conditions have not been reached.<sup>26</sup> On the other hand, conditions of complete depletion  
192 regime are clearly reached in the  $I_s$  around 5-10 nA as a constant product  $I_s \tau$  is  
193 obtained. When  $I_s > 10 \text{ nA}$ , the product  $I_s \tau$  decreases due to the lack of full depletion  
194 conditions (Fig. 1A). Below  $I_s = 5 \text{ nA}$ , despite corresponding to the complete depletion  
195 region, the product  $I_s \tau$  decreases because of the influence of oxygen and the chemical  
196 oxidation of other non-analyte metals dissolved in the sample (Fig. 1A).<sup>27</sup> In fact,  
197 electrons from the oxidation of  $M^0$  and from the discharging process (of the electrode  
198 acting as capacitor) are either consumed by the oxidants such as traces of oxygen or  
199 other interfering cations (also called electroless effect<sup>27</sup>) or fed to the potentiostat (as  $I_s$ ).  
200 Thus, the imposed stripping current ( $I_s > 0$ ) can be seen as the result of several  
201 components: the faradaic current ( $I_{\text{faradaic}} > 0$ , the one relevant for AGNES purposes), the  
202 current due to other oxidants ( $I_{\text{Ox}} < 0$ , that would also appear in the absence of analyte)  
203 and the capacitive current ( $I_{\text{cap}} > 0$ ).<sup>28</sup>

$$204 \quad I_s = I_{\text{faradaic}} + I_{\text{Ox}} + I_{\text{cap}} \quad (2)$$

205 As shown in the Supplementary data: i) measuring the area above the baseline in a  $dt/dE$   
206 vs  $E$  plot provides an analytical signal ( $\tau$ ) where the capacitive component has already  
207 been subtracted; ii) the rigorous expression for the faradaic current leads to the  
208 following expression for the charge:

$$209 \quad Q = (I_s - I_{Ox}) \tau \quad (3)$$

210 Since  $I_s > 0$  and  $I_{Ox} < 0$ , previous equation can be physically understood as the oxidants  
211 flux contributing (as “chemical stripping”) to the fixed  $I_s$ . So, in the reoxidation of the  
212 amalgamated metal the “effective” stripping current ( $I_s - I_{Ox}$ ) is larger than the nominal  
213  $I_s$ . Eq. 3 can be seen as equivalent (for this technique) to Eq. (9) in <sup>29</sup>.

214 The traditional product  $I_s \tau$  can be, therefore, corrected taking into account the  
215 contribution of these other oxidants present in the solution. One advantage of AGNES-  
216 SCP is that  $I_{Ox}$  can be easily measured in the waiting stage (i.e. quiescent solution),  
217 between the deposition with stirring and the stripping SCP stage. In this waiting stage, a  
218  $t_w$  of 50 s was found long enough for the practical extinction of the stirring effects. The  
219 measured current at the end of this stage, around -0.5 nA, can be used as  $I_{Ox}$  for the  
220 quantification of the SCP stage. The new corrected plot, representing the faradaic  
221 charge (Fig. 1B), shows how  $Q = (I_s - I_{Ox}) \tau$  stabilizes at 0.135  $\mu\text{C}$  even for the lowest  $I_s$   
222 values, which confirms that the oxidants contributions can be effectively assessed with  
223 the aforementioned procedure. For  $I_s > 10$  nA, complete depletion conditions are not  
224 achieved (Fig. 1B). This result has been validated against the stripped charge obtained  
225 ( $Q = 0.131 \mu\text{C}$ , see horizontal line) in classical AGNES with two pulses ( $Y_1 = 500$ ,  $t_{1,a} =$   
226  $350$  s,  $t_{1,b} = 1050$  s,  $Y_{1, sb} = 0.01$ ,  $Y_2 = 10^{-8}$ ).<sup>11</sup>

227 On this basis, a stripping current of 1 nA was chosen to perform SCP in AGNES with  
228 HMDE, because it corresponds to the horizontally stabilized charge in a region

229 sufficiently away from the  $I_s$ -interval where the computed charge decreases due to the  
230 lack of full depletion.

231

### 232 **3.2 Implementation of AGNES-SCP for SPE**

233 Preliminary studies have also been performed with SPE and stripping currents from 0.1  
234 nA to 50  $\mu$ A have been evaluated in a deaerated solution with  $c_{T,Zn} = 100 \text{ nmol L}^{-1}$ . The  
235 deposition stage was carried out with a gain  $Y = 5000$  and  $t_1 = 400 \text{ s}$ . These conditions  
236 have been previously determined in other published works.<sup>12</sup> The plot of  $I_s \tau^{1/2}$  never  
237 allowed to obtain a plateau whatever the  $I_s$  value (see supplementary data, Fig. S1),  
238 indicating that conditions of semi-infinite linear diffusion are not achieved. However,  
239 when a  $I_s$  in the range of 1 - 20  $\mu$ A is applied, the product  $I_s \tau$  is constant and, thus,  
240 under a complete depletion regime. Using these conditions, the slope of the potential  $E$   
241 versus time is the same before and after the oxidation which corresponds to a well-  
242 defined baseline.<sup>26</sup> All results indicate that a SPE behaves as a microelectrode for which  
243 practically achievable conditions always correspond to the complete depletion regime.<sup>30</sup>  
244 For  $I_s$  lower than 100 nA, the product  $I_s \tau$  decreases as the contribution of the other  
245 oxidants dissolved in the solution starts being noticeable. A stripping current of 10  $\mu$ A  
246 was retained, since the total accumulated charge is measured and there is no need to  
247 apply any oxidants correction as they can be considered negligible ( $I_{Ox} \ll I_s$ ).

248

### 249 **3.3 Calibrations of $Zn^{2+}$ , $Cd^{2+}$ and $Pb^{2+}$ in a solution containing only** 250 **one metal**

251 Analytical performances of AGNES-SCP with HMDE and SPE have been estimated  
252 from calibration curves based on triplicate analyses of each concentration level. These  
253 experiments have been carried out by using the conditions previously determined for

254 each working electrode (for HMDE,  $Y = 500$ ,  $t_{1,a} = 350$  s,  $t_{1,b} = 1050$  s and  $I_s = 1$  nA; for  
255 SPE,  $Y = 5000$ ,  $t_1 = 400$  s and  $I_s = 10$   $\mu$ A) regardless of the studied metal. The  
256 calibration plots have been performed using the accumulated charge  $Q$  which has been  
257 computed from the transition time  $\tau$  obtained during the SCP stage. A good linearity  
258 between charge and free concentration has been obtained for  $Zn^{2+}$ ,  $Cd^{2+}$  and  $Pb^{2+}$  with  
259 both HMDE and SPE. However, as expected when working with HMDE, since the  
260 applied  $I_s$  is very low, the current due to other oxidants ( $I_{ox} \approx -0.5$  nA) becomes of great  
261 relevance and its inclusion to compute to the faradaic charge (Eq. 3) yields a significant  
262 improvement of the results (see Table 1 and Fig. S2 in supplementary information).  
263 Thus, the retrieved experimental  $h_Q$  values for HMDE (with the oxidants correction)  
264 and SPE in all the performed calibrations agree favourably with theoretical ones, which  
265 can be estimated from the mercury volume  $V_{Hg}$ , the number of exchanged electrons ( $n =$   
266 2) and the Faraday constant:

$$267 \quad h_Q = nFV_{Hg}Y \quad (4)$$

268 Using Eq. 4, we obtain  $h_Q = 1.14$  C/(mol L<sup>-1</sup>) for HMDE with  $Y = 500$  and  $h_Q = 1.85$   
269 C/(mol L<sup>-1</sup>) for SPE with  $Y = 5000$ . The higher sensitivity of SPE is linked to a higher  
270 value of the product of the mercury volume ( $1.9 \times 10^{-6}$  m<sup>3</sup>) times the applied gain. The  
271 normalized sensitivity  $\eta_Q = h / Y$  (Tables 1 and 2) for an electrode type (and various  
272 metals) is approximately constant, indicating an approximate constancy in the volumes  
273 of Hg of each type of electrode. The specific values of  $\eta_Q$  found with AGNES-SCP  
274 (Tables 1 and 2) are in good agreement with those previously published.<sup>11, 12</sup>

275 The limits of detection (LOD) have been statistically calculated for  $Zn^{2+}$ ,  $Cd^{2+}$  and  $Pb^{2+}$   
276 and both working electrodes as

$$277 \quad LOD = \frac{kS_b}{m} \quad (5)$$

278 where  $k = 3$ ,  $S_b$  is the intercept standard deviation of the regression line and  $m$  is the  
279 slope of the calibration graph. The limits of quantification (LOQ) were calculated  
280 through the same equation as for the LOD, with the constant  $k = 10$ . Values of LOD and  
281 LOQ are also gathered in Table 1. Limits of detection obtained for a preconcentration  
282 factor of 500 and 5000, for HMDE and SPE respectively, appeared in the  $\text{nmol L}^{-1}$   
283 range, which is of the same order as those obtained with classical SCP in the study of  
284 labile trace metals.<sup>23</sup> LOD and LOQ obtained for SPE are lower than HMDE ones  
285 (Table 1). Together with the required shorter deposition times, it clearly highlights the  
286 extraordinary performance of the screen-printed electrodes.

287

### 288 **3.4 Interference study in a mixture of metals**

289 Since many systems, such as natural waters, are mixtures of different metals, we turn  
290 now our attention to possible interferences. In other published work<sup>12</sup>, it has been shown  
291 that using the charge as response function of AGNES, with a fixed stripping potential  
292 (not in the diffusion limited conditions) as second stage, can overcome some difficulties  
293 in complex samples, for example, Cd in presence of Pb. The strategy of adapting the  
294 stripping potential is efficient, provided that the supply of Pb to the electrode (e.g. either  
295 from free Pb or from labile and mobile complexes) is limited. In some cases (e.g.  
296  $c_{\text{T,oxalate}} = 0.02 \text{ mol L}^{-1}$ ,  $c_{\text{T,Cd}} = c_{\text{T,Pb}} = 3 \text{ } \mu\text{mol L}^{-1}$ ,  $\text{pH} = 6$ ) the measurement was not even  
297 possible. Moreover, the presence of interferent metal ions can hinder the finding of  
298 suitable blanks and consequently the determination of the capacitive current.

299 First, the suitability of SCP as the stripping step of AGNES was checked by using a  
300 SPE as working electrode. The free Cd analytical signal obtained for a total Cd  
301 concentration of  $100 \text{ nmol L}^{-1}$  has been followed by adding increasing concentrations of  
302 Pb (from 50 to  $500 \text{ nmol L}^{-1}$ ). The same experimental conditions as those previously

303 determined for the monometallic study have been used. As shown in Fig. 2, the peaks  
304 corresponding to Cd and Pb were clearly discriminated, although a gradual positively  
305 shift of the Cd peak potential was observed when increasing Pb concentration.  
306 Nevertheless, there was no difficulty in computing the Cd<sup>2+</sup> reoxidation time  $\tau$  which  
307 equals to  $21.3 \pm 0.6$  ms.

308 The ability of SCP as second stage of AGNES to handle interferences has been then  
309 evaluated by carrying out calibrations of Zn<sup>2+</sup>, Cd<sup>2+</sup> and Pb<sup>2+</sup> with HMDE and SPE in a  
310 mixture of the three aforementioned metals. AGNES-SCP has been sequentially applied  
311 to each metal (e.g. first with AGNES deposition potential for Zn, then for Cd and finally  
312 for Pb) at each calibration point in a solution where the 3 metals reached the same total  
313 concentration. The same experimental conditions as those used for monometallic study  
314 have been applied and the oxidants correction has also been taken into account when  
315 using HMDE as working electrode. As shown in Fig. 3, in all the performed  
316 experiments, well shaped peaks were obtained whatever the analysed metal. As in the  
317 monometallic study, a good linearity has been obtained between accumulated charge  
318 and  $[M^{2+}]$  (data not shown). The obtained sensitivities  $h_Q$  (Table 2) appeared very  
319 similar to those obtained in a solution containing only one metal (Table 1), which  
320 indicated that the interferences are negligible on the three metal measurements,  
321 regardless the working electrode.

322

### 323 **3.5 Speciation results**

324 With HMDE and AGNES-SCP, we have tackled a system that could not be analyzed  
325 with a fixed potential in the stripping stage: total cadmium of  $3 \mu\text{mol L}^{-1}$  and oxalate  
326  $0.02 \text{ mol L}^{-1}$  at a fixed pH of 6, in presence of increasing Pb concentrations. Two  
327 replicates for three different Pb additions, from 1 to  $4.5 \mu\text{mol L}^{-1}$ , were performed in

328 order to check its influence on the determination of  $[\text{Cd}^{2+}]$ . When applying AGNES  
329 variant with two pulses ( $E_1 \approx -0.63$  V,  $E_2 \approx -0.51$  V and a shifted blank with  $E_{1,\text{sb}} \approx -0.28$   
330 V and  $E_{2,\text{sb}} \approx -0.17$  V to avoid  $\text{Pb}^0$  deposition and reoxidation), the apparent free Cd  
331 concentration increased linearly with each Pb addition (see Fig. S3 in supplementary  
332 data). The reason of this undesirable increase is that, when applying  $E_1$ , not only  $\text{Cd}^0$  is  
333 preconcentrated, but also  $\text{Pb}^0$  and both metals are, thus, reoxidated and quantified  
334 together during the stripping stage. On the other hand, AGNES-SCP allowed measuring  
335 the free cadmium concentration in the same aforementioned samples with no influence  
336 of the Pb interference, since SCP separates the signals of Cd and Pb reoxidation. The  
337 experimental settings have been  $Y = 500$ ,  $t_1 = 300$  s and  $I_s = 1$  nA. The deposition time  $t_1$   
338 could be reduced taking advantage of the presence of labile oxalate complexes that  
339 contribute to the flux.<sup>31</sup> However, in these experiments, a special situation has been  
340 found where determining the typical reoxidation time  $\tau$  was a challenge as a “distorted”  
341 stripping  $dt/dE$  peak was obtained (Fig. 4). The baseline of these peaks at the more  
342 negative potential could not be recognized. In these cases, we suggest to first compute  
343 the total area under the metal peak (thus, including the capacitive current). This total  
344 area is called  $\tau'$  in order to distinguish from  $\tau$ , which is typically determined by  
345 integrating the peak area above the baseline (Fig. 4). Then, the capacitive contribution  
346 can be subtracted from  $\tau'$  (see mathematical details and the underlying assumptions in  
347 supporting data) to calculate  $\tau$ . With this methodology, a free metal concentration of  $83$   
348  $\pm 1$  nmol L<sup>-1</sup> ( $n = 8$ ) has been obtained, indicating that the successive Pb additions have  
349 not hindered the proper measurement of  $[\text{Cd}^{2+}]$ . The oxidants correction was also  
350 crucial. These results have been validated using a Cd-ISE, obtaining a free cadmium  
351 concentration of  $82 \pm 1$  nmol L<sup>-1</sup>, which is very similar to the one measured with  
352 AGNES (Fig. S3). These experiments are a relevant achievement of AGNES-SCP,



353 since this interference could not be avoided when the second stage of AGNES was  
354 performed with a fixed stripping potential.

355 Finally, the performances of AGNES-SCP have been checked with a SPE, by carrying  
356 out a speciation experiment of Cd in a  $\text{KNO}_3$  solution containing different NTA  
357 concentrations at pH 4.8. Prior to the speciation experiment, a calibration was carried  
358 out in solutions with total Cd concentration from 50 to 200  $\text{nmol L}^{-1}$  (and no NTA) by  
359 plotting the faradaic charges against the free Cd concentrations computed with Visual  
360 Minteq.<sup>32</sup> Fig. 5 shows that experimental values obtained with SPE agreed well with the  
361 theoretical ones.

362

#### 363 **4. Conclusions**

364 SCP has been used as the second stage of AGNES, allowing the determination of free  
365 Zn, Cd and Pb concentrations in aqueous samples. AGNES-SCP has been implemented  
366 not only for the hanging mercury drop electrode, but also for the screen printed one,  
367 which paves the way to further *in situ* analysis. It has been found that stripping currents  
368 of  $I_s=1$  nA, for HMDE, and  $I_s=10$   $\mu\text{A}$ , for SPE, are suitable to work in the required full  
369 depletion regime. LOD close to the  $\text{nmol L}^{-1}$  were obtained for Zn, Cd and Pb with both  
370 kinds of electrodes, with good reproducibility. However, SPE appeared particularly  
371 promising because of the shorter electrodeposition time needed to reach these low  
372 concentrations.

373 The rigorous computation of the stripped faradaic charge from the recorded evolution of  
374 the potential is crucial in retrieving physicochemically sound calibration constants  $h_Q$ .

375 This computation requires: i) A suitable reading of  $\tau$ , which has been customarily taken  
376 as the area above the baseline in a  $dt/dE$  representation. However, when a large  
377 cadmium concentration ( $1 \mu\text{mol L}^{-1}$ ) and oxalate ( $0.02 \text{ mol L}^{-1}$ ) are present in a sample

378 at pH 6 and a low stripping current is applied (1 nA), metal peaks appear distorted and  $\tau$   
379 is not easy to compute. Then, the reading of  $\tau$  procedure can be generalized by  
380 measuring the total area under the  $dt/dE$  vs  $E$  peak (called  $\tau'$ ), and then subtracting the  
381 capacitive component. ii) The taking into account of the oxidants correction; which  
382 consists in measuring  $I_{Ox}$  at the end of the deposition stage under quiescent conditions  
383 and to subtract it from  $I_s$ . The oxidants correction can allow to work with lower  $I_s$ ,  
384 which yield larger transition times and improved accuracies. SPE uses so high stripping  
385 currents that, in most cases, this correction is negligible.

386 AGNES-SCP represents an important improvement over other AGNES variants, as it  
387 allows working easily in a large range of analyte concentrations, blanks can be spared  
388 and metal interferences are easily avoided. Different calibrations and studies with  
389 various mixtures of metals or ligands (NTA and oxalate) have been carried out and  
390 shown that the combination of SCP with AGNES is a technique suitable to handle  
391 interferences and to measure free metal ion concentrations properly.

392

### 393 **Acknowledgements**

394 The authors thank Dr. Jose Paulo Pinheiro for being the first to suggest the possibility of  
395 using SCP as the second stage of AGNES. The authors acknowledge support of this  
396 research from the Communauté d'Agglomération de Pau Pyrénées (CDAPP), from the  
397 Spanish *Ministerio de Ciencia e Innovación* (CTQ2009-07831 and CTQ2009-14612),  
398 from the European Community EFA15/08 (PyrMet) and from the *Comissionat*  
399 *d'Universitats i Recerca de la Generalitat de Catalunya* (2009SGR00465).

400

401 **References**

- 402 1. F. M. M. Morel, *Principles of aquatic chemistry*, John Wiley & Sons, New  
403 York, 1983.
- 404 2. P. G. C. Campbell, in *Metal speciation and bioavailability in aquatic systems*,  
405 eds. A. Tessier and A. P. F. Turner, Wiley & Sons Ltd, 1995, pp. 45-102.
- 406 3. M. Pesavento, G. Alberti and R. Biesuz, *Analytica Chimica Acta*, 2009, **631**,  
407 129-141.
- 408 4. E. J. J. Kalis, Weng, E. J. M. Temminghoff and W. H. van Riemsdijk, *Analytical*  
409 *Chemistry*, 2007, **79**, 1555-1563.
- 410 5. S. Noël, M.-L. Tercier-Waeber, L. Lin, J. Buffle, O. Guenat and M. Koudelka-  
411 Hep, *Electroanalysis*, 2006, **18**, 2061-2069.
- 412 6. N. Parthasarathy and J. Buffle, *Analytica Chimica Acta*, 1994, **284**, 649-659.
- 413 7. P. Buhlmann, E. Pretsch and E. Bakker, *Chem. Rev.*, 1998, **98**, 1593-1687.
- 414 8. J. Galceran, E. Companys, J. Puy, J. Cecilia and J. L. Garces, *Journal of*  
415 *Electroanalytical Chemistry*, 2004, **566**, 95-109.
- 416 9. J. Galceran, C. Huidobro, E. Companys and G. Alberti, *Talanta*, 2007, **71**, 1795-  
417 1803.
- 418 10. D. Chito, J. Galceran and E. Companys, *Electroanalysis*, 2010, **22**, 2024-2033.
- 419 11. J. Galceran, D. Chito, N. Martínez-Micaelo, E. Companys, C. David and J. Puy,  
420 *Journal of Electroanalytical Chemistry*, 2010, **638**, 131-142.
- 421 12. C. Parat, D. Aguilar, L. Authier, M. Potin-Gautier, E. Companys, J. Puy and J.  
422 Galceran, *Electroanalysis*, 2011, **23**, 619-627.
- 423 13. E. Companys, J. Puy and J. Galceran, *Environmental Chemistry*, 2007, **4**, 347-  
424 354.

- 425 14. J. Puy, J. Galceran, C. Huidobro, E. Companys, N. Samper, J. L. Garcés and F.  
426 Mas, *Environmental Science & Technology*, 2008, **42**, 9289-9295.
- 427 15. R. F. Domingos, C. Huidobro, E. Companys, J. Galceran, J. Puy and J. P.  
428 Pinheiro, *Journal of Electroanalytical Chemistry*, 2008, **617**, 141-148.
- 429 16. F. Zavarise, E. Companys, J. Galceran, G. Alberti and A. Profumo, *Analytical  
430 and Bioanalytical Chemistry*, 2010, **397**, 389-394.
- 431 17. C. M. A. Brett, A. M. O. Brett and L. Tugulea, *Analytica Chimica Acta*, 1996,  
432 **322**, 151-157.
- 433 18. M.-L. Tercier and J. Buffle, *Analytical Chemistry*, 1996, **68**, 3670-3678.
- 434 19. R. M. Town and H. P. van Leeuwen, *Journal of Electroanalytical Chemistry*,  
435 2002, **523**, 1-15.
- 436 20. D. Jagner, *Analyst*, 1982, **107**, 593-599.
- 437 21. N. Serrano, J. M. Díaz-Cruz, C. Ariño and M. Esteban, *Electroanalysis*, 2006,  
438 **18**, 955-964.
- 439 22. C. Parat, L. Authier, S. Betelu, N. Petrucciani and M. Potin-Gautier,  
440 *Electroanalysis*, 2007, **19**, 403-406.
- 441 23. C. Parat, A. Schneider, A. Castetbon and M. Potin-Gautier, *Analytica Chimica  
442 Acta*, 2011, **688**, 156-162.
- 443 24. O. Zaouak, L. Authier, C. Cugnet, A. Castetbon and M. Potin-Gautier,  
444 *Electroanalysis*, 2010, **22**, 1151-1158.
- 445 25. E. Companys, J. Cecilia, G. Codina, J. Puy and J. Galceran, *Journal of  
446 Electroanalytical Chemistry*, 2005, **576**, 21-32.
- 447 26. R. M. Town and H. P. van Leeuwen, *Journal of Electroanalytical Chemistry*,  
448 2001, **509**, 58-65.

- 449 27. R. M. Town and H. P. van Leeuwen, *Journal of Electroanalytical Chemistry*,  
450 2004, **573**, 147-157.
- 451 28. A. J. Bard and L. R. Faulkner, *Electrochemical Methods: Fundamentals and*  
452 *Applications* 2nd edn., John Wiley & Sons, 2001.
- 453 29. C. Hua, D. Jagner and L. Renman, *Analytica Chimica Acta*, 1987, **197**, 257-264.
- 454 30. H. P. van Leeuwen and R. M. Town, *Journal of Electroanalytical Chemistry*,  
455 2002, **523**, 16-25.
- 456 31. G. Alberti, R. Biesuz, C. Huidobro, E. Companys, J. Puy and J. Galceran,  
457 *Analytica Chimica Acta*, 2007, **599**, 41-50.
- 458 32. J. D. Allison, D. S. Brown and K. J. Novo-Gradac, *MINTEQA2/PRODEFA2, A*  
459 *geochemical assessment model for environmental systems: version 3.0 user's*  
460 *manual*, Washington, DC, EPA/600/3-91/021, 1991.
- 461
- 462

463

**TABLE**

464

465 Table 1. AGNES-SCP performances obtained from a calibration with HMDE ( $Y=500$ ,466  $t_{1,a} = 350$  s,  $t_{1,b} = 1050$  s,  $I_s = 1$  nA) and SPE ( $Y = 5000$ ,  $t_1 = 400$ s,  $I_s = 10$   $\mu$ A) with five467 metal concentrations (between 25 and 100 nmol L<sup>-1</sup>) replicated three times.

468

		HMDE		SPE	
		from $I_s \tau$	from $Q=(I_s-I_{ox})\tau$	from $I_s \tau$	from $Q=(I_s-I_{ox})\tau$
Zn	Sensitivity $h_Q$ (C/(mol L <sup>-1</sup> ))	0.48±0.02	1.09±0.03	1.86±0.02	1.90±0.02
	$\eta_Q$ (C/(mol L <sup>-1</sup> ))	0.96×10 <sup>-3</sup>	2.18×10 <sup>-3</sup>	0.37×10 <sup>-3</sup>	0.38×10 <sup>-3</sup>
	LOD / (nmol L <sup>-1</sup> )	8.1	4.0	2.6	2.6
	LOQ / (nmol L <sup>-1</sup> )	27	13.4	8.6	8.5
Cd	Sensitivity $h_Q$ (C/(mol L <sup>-1</sup> ))	0.48±0.02	1.00±0.02	1.40±0.01	1.41±0.01
	$\eta_Q$ (C/(mol L <sup>-1</sup> ))	0.96×10 <sup>-3</sup>	2.00×10 <sup>-3</sup>	0.28×10 <sup>-3</sup>	0.28×10 <sup>-3</sup>
	LOD / (nmol L <sup>-1</sup> )	11.3	2.9	2.1	2.1
	LOQ / (nmol L <sup>-1</sup> )	37.5	9.8	7.0	6.9
Pb	Sensitivity $h_Q$ (C/(mol L <sup>-1</sup> ))	0.51±0.03	0.99±0.02	1.93±0.01	1.93±0.01
	$\eta_Q$ (C/(mol L <sup>-1</sup> ))	1.02×10 <sup>-3</sup>	1.98×10 <sup>-3</sup>	0.39×10 <sup>-3</sup>	0.39×10 <sup>-3</sup>
	LOD / (nmol L <sup>-1</sup> )	7.7	4.1	1.1	1.1
	LOQ / (nmol L <sup>-1</sup> )	25.6	13.6	3.7	3.6

469

470

471 Table 2. Values of the proportionality factors,  $h_Q$  and  $\eta_Q = h_Q/Y$  (in  $C/(\text{mol L}^{-1})$ ),  
472 obtained in linear regressions of calibrations with HMDE and SPE in solutions  
473 containing a mixture of the 3 metals with equal concentrations. HMDE:  $Y = 500$ ,  $t_{1a} =$   
474  $350$  s,  $t_{1b} = 1050$  s,  $I_s = 1$  nA; SPE:  $Y = 5000$ ,  $t_1 = 400$ s,  $I_s = 10$   $\mu$ A. Means and standard  
475 deviations correspond to a calibration performed with 5 concentrations (between 0 and  
476  $100$  nmol  $L^{-1}$ ) replicated 3 times.

477

	HMDE			SPE		
	$h_Q$ $C/(\text{mol L}^{-1})$	$\eta_Q$ $C/(\text{mol L}^{-1})$	$\eta_Q^{12}$ $C/(\text{mol L}^{-1})$	$h_Q$ $C/(\text{mol L}^{-1})$	$\eta_Q$ $C/(\text{mol L}^{-1})$	$\eta_Q^{12}$ $C/(\text{mol L}^{-1})$
<b>Zn</b>	$1.13 \pm 0.02$	$2.22 \times 10^{-3}$	$2.32 \times 10^{-3}$	$1.95 \pm 0.02$	$0.39 \times 10^{-3}$	$0.33 \times 10^{-3}$
<b>Cd</b>	$0.99 \pm 0.03$	$1.98 \times 10^{-3}$	$2.27 \times 10^{-3}$	$1.45 \pm 0.01$	$0.29 \times 10^{-3}$	$0.32 \times 10^{-3}$
<b>Pb</b>	$0.98 \pm 0.02$	$1.96 \times 10^{-3}$	$2.42 \times 10^{-3}$	$2.47 \pm 0.03$	$0.49 \times 10^{-3}$	$0.32 \times 10^{-3}$

478

479

480 **FIGURE Caption**

481 Figure 1. A) Behaviour of  $I\tau$  (○) and  $I\tau^{1/2}$  (×) obtained with a HMDE and B) Stripped  
482 charge, applying the oxidants correction shown in Eq. (3). The red horizontal line  
483 indicates the charge computed when the stripping stage is a fixed potential pulse under  
484 diffusion limited conditions (classical AGNES).  $c_{T,Zn} = 10 \text{ nmol L}^{-1}$ ,  $[\text{KNO}_3] = 0.1 \text{ mol}$   
485  $\text{L}^{-1}$ ,  $Y = 500$ ,  $t_{1,a} = 350 \text{ s}$  and  $t_{1,b} = 1050 \text{ s}$ .  $I_s$  from 0.01 to 100 nA.

486

487 Figure 2. Cd peaks obtained during the oxidation step in AGNES-SCP with a SPE in a  
488 solution containing  $c_{T,Cd} = 100 \text{ nmol L}^{-1}$  and increasing  $c_{T,Pb}$  concentrations from 50 to  
489  $500 \text{ nmol L}^{-1}$ .  $[\text{KNO}_3] = 0.1 \text{ mol L}^{-1}$ ,  $Y = 5000$ ,  $t_1 = 400 \text{ s}$ ,  $I_s = 10 \mu\text{A}$ .

490

491 Figure 3. Sequential analysis of  $[\text{Zn}^{2+}]$ ,  $[\text{Cd}^{2+}]$  and  $[\text{Pb}^{2+}]$  by using AGNES-SCP method  
492 with a HMDE for Zn, Cd and Pb total concentrations of 0, 25; 50, 75 and  $100 \text{ nmol L}^{-1}$ .  
493  $[\text{KNO}_3] = 0.1 \text{ mol L}^{-1}$ ,  $Y = 500$ ,  $t_{1a} = 350 \text{ s}$ ,  $t_{1b} = 1050 \text{ s}$ ,  $I_s = 1 \text{ nA}$ .

494

495 Figure 4. Stripping  $dt/dE$  vs  $E$  plot, in HMDE with  $Y = 500$ ,  $t_1 = 300 \text{ s}$  and  $I_s = 1 \text{ nA}$ , of a  
496 solution with total Cd and Pb concentrations of  $3 \mu\text{mol L}^{-1}$  and total oxalate of  $0.02 \text{ mol}$   
497  $\text{L}^{-1}$  at  $\text{pH} = 6$ . The total shaded area is called  $\tau'$ ; being  $\tau$  the area above the dashed line  
498 and the capacitive component the area below the dashed line.

499

500 Figure 5. Free Cd concentration variations in a  $0.1 \text{ mol L}^{-1} \text{ KNO}_3$  solution containing a  
501 total Cd concentration of  $200 \text{ nmol L}^{-1}$  and NTA from 0 to  $31 \mu\text{mol L}^{-1}$  at  $\text{pH} 4.8$ ,  
502 determined by AGNES-SCP with a SPE (circle marker, ○) and predicted by Visual  
503 MINTEQ (square marker, ■).  $Y = 5000$ ,  $t_1 = 400 \text{ s}$  and  $I_s = 10 \mu\text{A}$ .

504



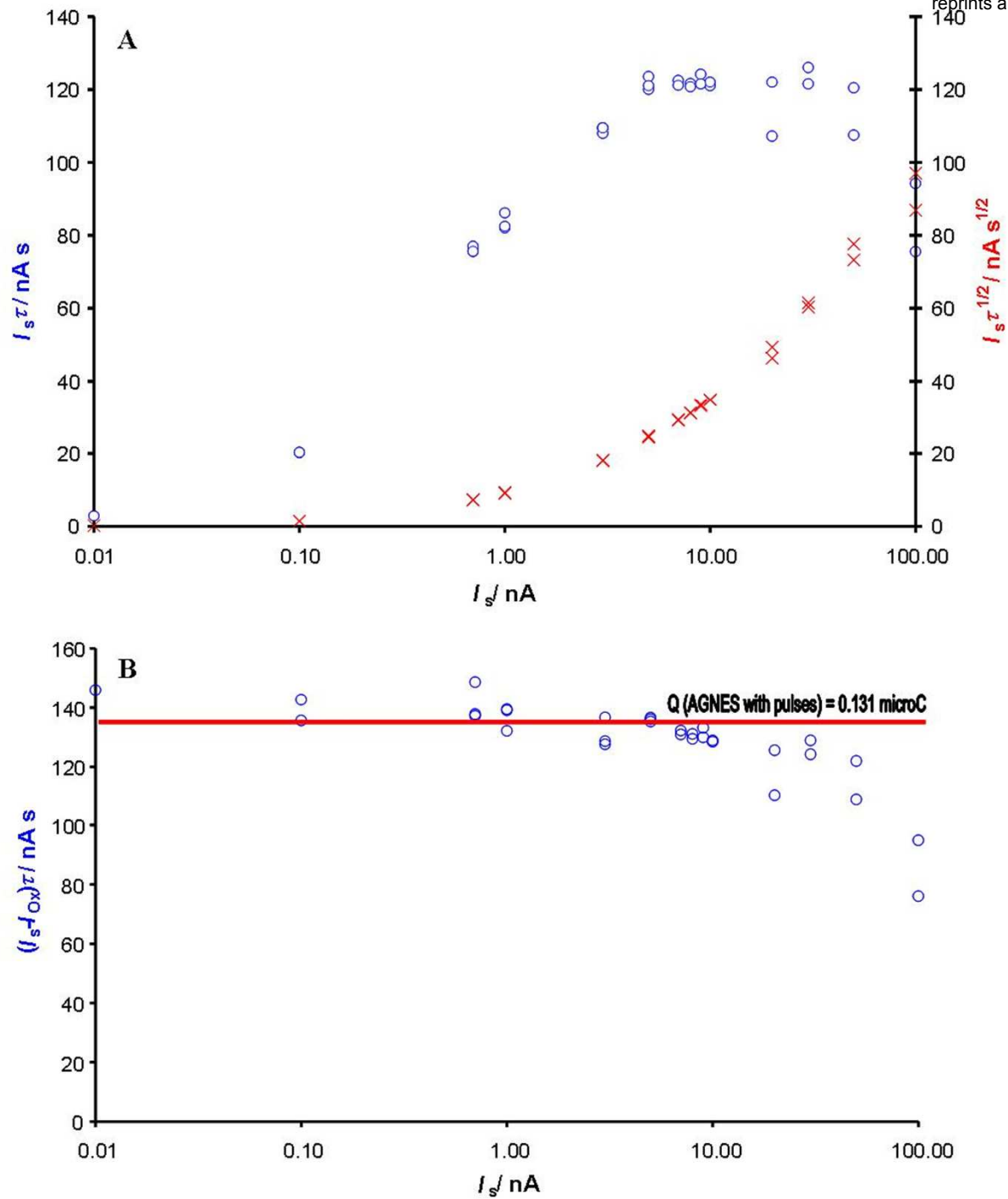


Fig 1

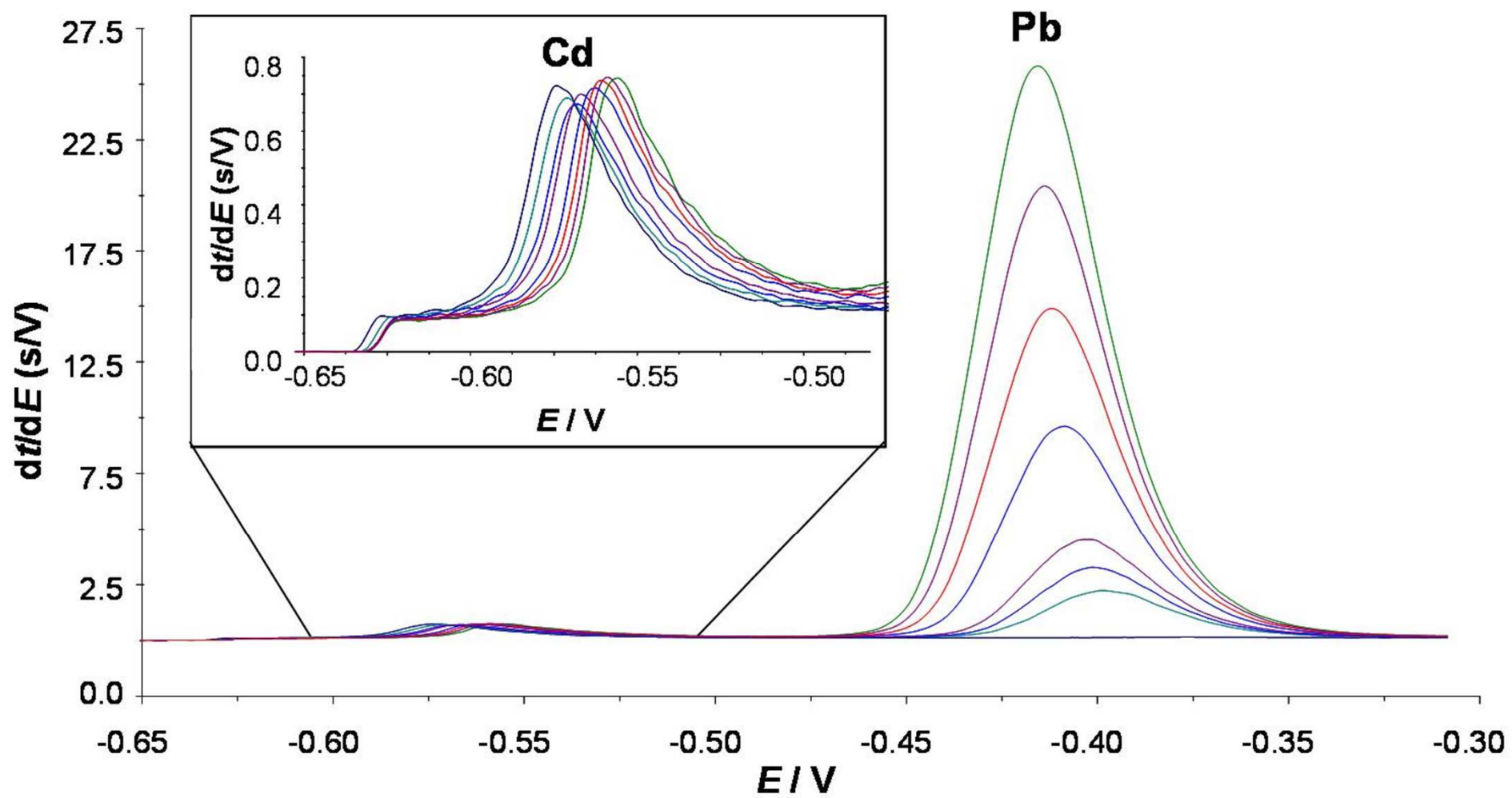


Fig 2

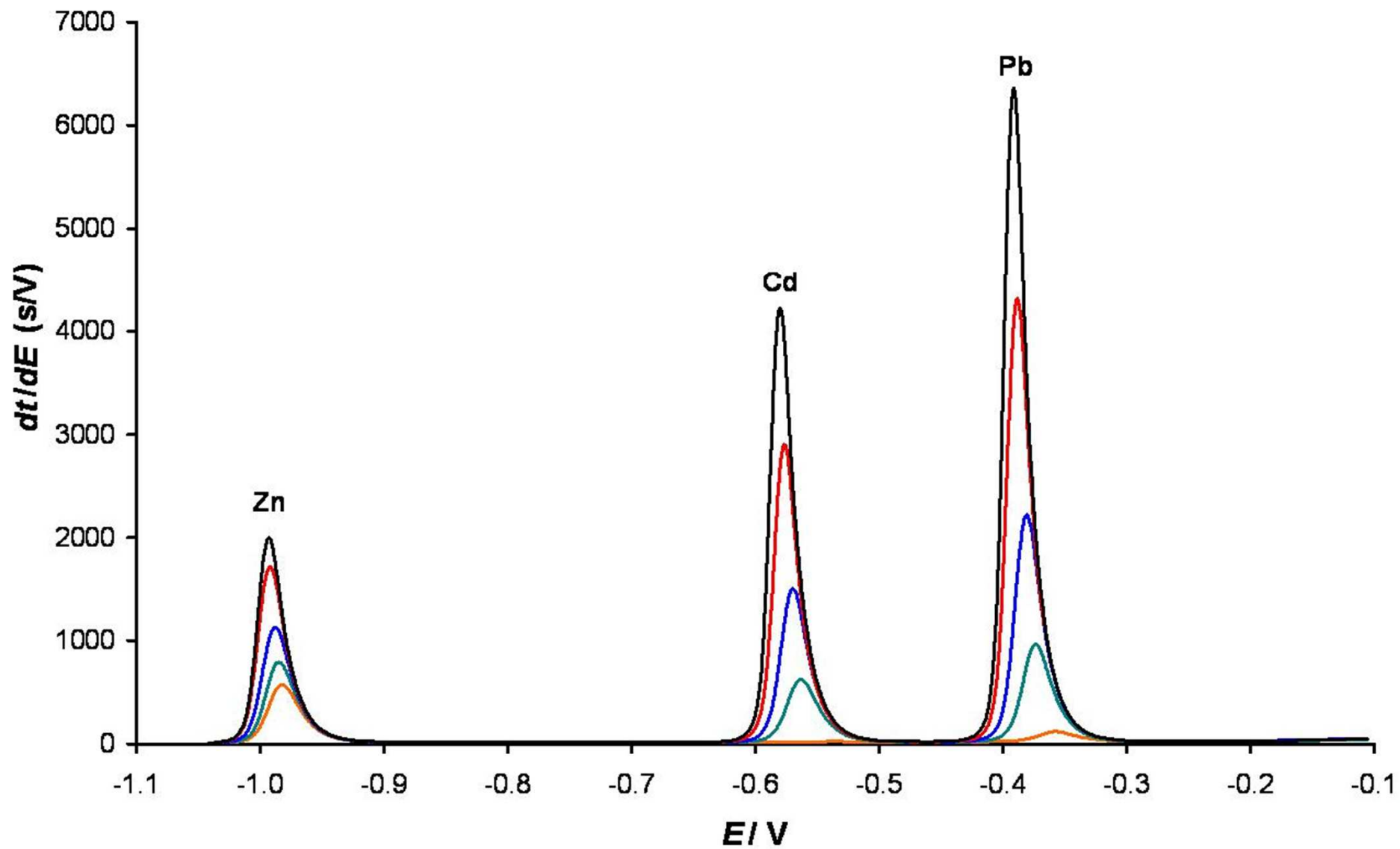


Fig 3

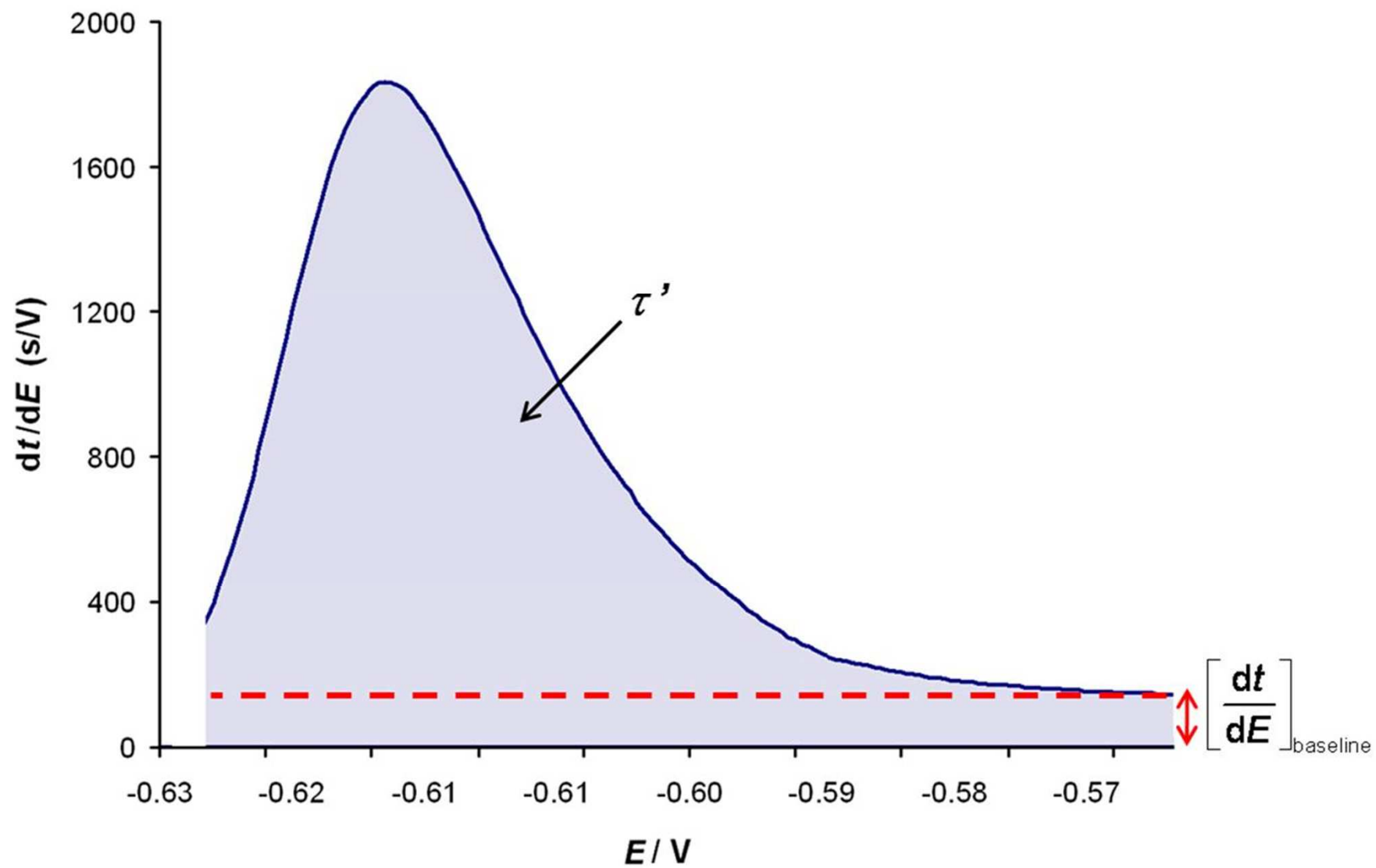


Fig 4

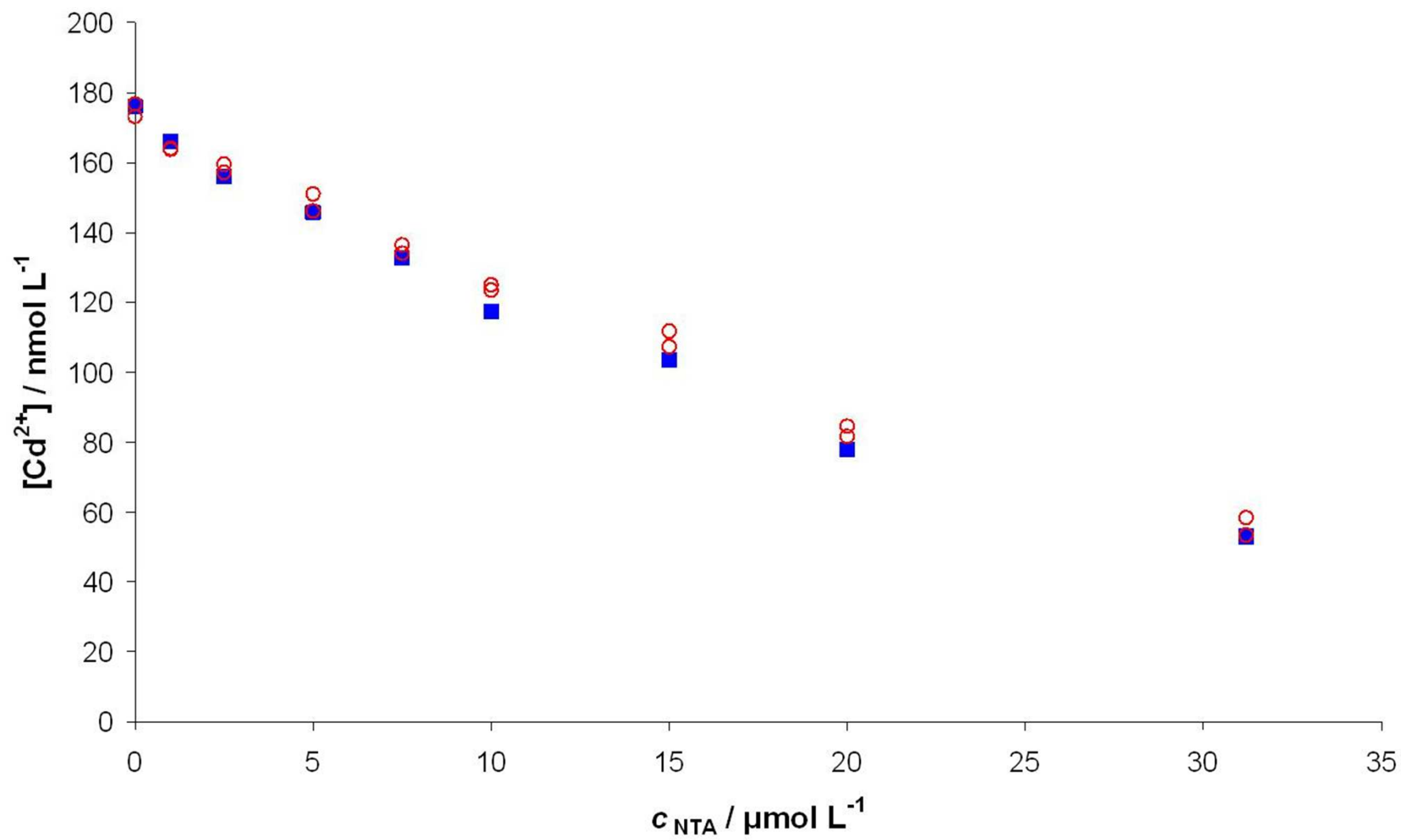


Fig 5